Untangling the role of biotic and abiotic ageing of various environmental plastics toward the sorption of metals

Gilberto Binda [a,*], Margarida Costa [a], Luka Supraha [a], Davide Spanu [b], Christian Vogelsang [a], Eva Leu [c], Luca Nizzetto [a,d]

[a] *Norwegian Institute for Water Research (NIVA), Økernveien 94, 0579 Oslo, Norway*
[b] *Department of Science and High Technology, University of Insubria, Via Valleggio 11, 22100 Como, Italy*
[c] *Akvaplan-niva, Fram Centre, 9296 Tromsø, Norway*
[d] *RECETOX, Masaryk University, Kamenice 753/5, 625 00 Brno, Czech Republic*

HIGHLIGHTS

- The effects of plastic polymers and ageing processes on metal sorption are tested.
- All ageing processes alter the surface properties of plastic.
- Only biofouling significantly increases metal sorption on plastic.
- The environmental consequences of plastic biotic ageing need further investigations.

GRAPHICAL ABSTRACT
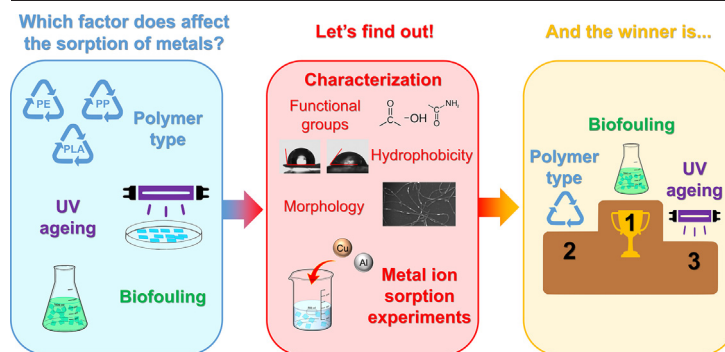
ARTICLE INFO

ABSTRACT

Plastic particles can impact the environmental fate and bioavailability of essential inorganic micronutrients and non-essential (toxic) metals. The sorption of metals to environmental plastic has been demonstrated to be facilitated by plastic ageing, a phenomenon encompassing an array of physical, chemical, and biological processes. This study deploys a factorial experiment to untangle the role of different ageing processes in determining the sorption of metals. Plastics made of three different polymer types were aged both through abiotic (ultraviolet irradiation, UV) and biotic (through the incubation with a multispecies algal inoculum forming a biofilm) processes under controlled laboratory conditions. Pristine and aged plastic samples were characterized for their physiochemical properties through Fourier-transformed infrared spectroscopy, scanning electron microscopy and water contact angle measurements. Their sorption affinity toward aluminum (Al) and copper (Cu) in aqueous solutions was then assessed as a response variable. All ageing processes (alone or combined) influenced plastic surface properties resulting in reduced hydrophobicity, changes in surface functional groups (i.e., increase of oxygen containing functional groups after UV ageing and the appearance of marked bands as amides and polysaccharides after biofouling), as well as in nanomorphology. The sorption of Al and Cu was instead statistically dependent ($p < 0.01$) on the degree of biofouling covering the specimens. Biofouled plastic displayed in fact substantial affinity for metal sorption causing the depletion of up to tenfold Cu and Al compared to pristine polymers, regardless of the polymer type and presence or absence of other ageing treatments. These results confirm the hypothesis that the accumulation of metals on plastic is substantially driven by the

* Corresponding author.
  E-mail address: gilberto.binda@niva.no (G. Binda).

biofilm present on environmental plastics. These findings also highlight the importance of investigating the implications of environmental plastic for metal and inorganic nutrients availability in environments impacted by this pollution.

1. Introduction

The interactions of (micro)plastic with metals have recently gained attention of researchers owing to the possible environmental toxicological and/or ecological implications (Binda et al., 2021; Cao et al., 2021). Evidences from laboratory studies highlighted the potential for sorption of some dissolved metals in water solution by environmental plastic (Hildebrandt et al., 2021; Holmes et al., 2012). If such interactions happen also in the environment, plastic polluted ecosystems (e.g., floodplains and freshwater bodies, Bellasi et al., 2020) can potentially influence the availability of micronutrients and toxic metals (Bradney et al., 2019; Conan et al., 2022; Seeley et al., 2020).

The environmental ageing of plastic has been pointed out as a key process for the sorption of metals (Binda et al., 2023a; Kalčíková et al., 2020; Lang et al., 2020). Ageing encompasses a complex array of physical, chemical, and biological processes which affect the properties of environmental plastic (Bellasi et al., 2022; Sun et al., 2020; Wang et al., 2023). Abiotic (physical and chemical) ageing processes, for example, change of the surface chemical characteristics through the increase of oxygen-containing functional groups (e.g., carbonyl and hydroxyl groups Koelmans et al., 2019; Liu et al., 2021c), affecting in turn surface charge and hydrophobicity. These processes can also enhance polymer chain fracturing, resulting in fragmentation and increased surface area per unit of plastic volume. This can lead to increased affinity of plastic toward metal sorption (Wang et al., 2020). Biotic processes also affect plastic affinity for dissolved metals. Beyond the ecological implications of plastic colonization by microorganisms such as bacteria, algae and fungi (Amaral-Zettler et al., 2020), the formation of the so-called "eco-corona" on plastic also affects its surface properties by changing surface functional groups and surface charge (Binda et al., 2023b; El Hadri et al., 2020; Rozman et al., 2023; Witzmann et al., 2022; Wright et al., 2020).

Several recent studies observed the enhanced sorption of (trace) metals on plastic after their environmental (on site) or controlled ageing (in laboratory) and considering a wide range of polymer types: biotic and abiotic ageing processes seem to play a pivotal role (Bhagwat et al., 2021; Guan et al., 2020; Li et al., 2022a; Liu et al., 2021b; Liu et al., 2021a; Stabnikova et al., 2022). However, the prevalent ageing processes controlling this effect and the underlying changes in plastic physiochemical properties have not yet been identified, after statistically factoring-out the possible main confounders.

In this study we aim at systematically assessing how different factors affect surface properties of plastic and in turn define the capacity for the sorption of metals in water. To this end, a factorial experimental design was deployed considering the following four factors: i) polymer composition (polyethylene, PE; polypropylene, PP; and polylactic acid, PLA), ii) abiotic ageing level (treatments with and without ultraviolet (UV) induced oxidation), iii) biotic ageing (presence and absence of biofilm), iv) abiotic and biotic (UV ageing and biofouling) in combination. As response variables we considered the sequestration on the plastic surface of two target metals (aluminum, Al and copper, Cu) added in solution in the ionic form, as well as the changes in the physicochemical surface properties of plastic. The main objective of the experiment was to test the hypothesis that biofouling is the prevalent factor controlling sorption of metals onto plastics. Aluminum and Cu were selected for their critical role at minor and trace concentration in water environments: they can be naturally present in water bodies at (trace) levels, but can present toxic activities at increasing concentration; they can serve as examples of essential (Cu) and non-essential (Al) metals commonly present in water environments; they also present different chemical speciation in water bodies (Botté et al., 2022;

Gaetke, 2003; Ndungu, 2012; Silva Pinheiro et al., 2020). In addition, these elements have recently been found associated to environmental plastic samples (Binda et al., 2023a; Johansen et al., 2019; Richard et al., 2019; Xie et al., 2021). As a secondary objective we also tested how different plastic polymers and UV ageing affect the formation of a biofilm community on its surface. The tested factors were the polymer type (PE, PP, PLA) and the UV ageing process.

2. Materials and methods

2.1. Plastic samples and reagents

Plastic samples were obtained from commercial objects by cutting "confetti-like" fragments of different polymers (PP, PE and PLA) in squares of about 5 × 5 mm with variable thickness (0.05 mm for PE and 0.3 mm for PP and PLA). Single-use transparent lids for food were used to create PP (Pro-Pac, Germany) and PLA fragments (PAPSTAR, Germany), while PE fragments were obtained from a black agricultural mulching film (information on the manufacturer cannot be disclosed, but details on main physico-chemical properties can be found in Hurley et al., 2023).

All solutions were prepared using ultrapure water (18.2 MΩ x cm resistivity) obtained from a Sartorius (Germany) Arium™ pro VF. Aluminum and Cu stock solutions (1 g/l) were made by dissolution of solid $Al_2(SO_4)_3 \cdot H_2O$ (Sigma Aldrich, United States of America) and $CuSO_4 \cdot 5H_2O$ (Merck, Germany). $NaNO_3$ and NaOH used for solution buffering were obtained by the dissolution of solid $NaNO_3$ and NaOH pills (Merck, Germany) in distilled water. Algal growth medium was prepared following the Z8 recipe (Kotai, 1972). All solid reagents were of reagent-grade purity. Nitric acid for labware washing and pH buffers was obtained by dilution of HNO_3 Suprapur (Sigma Aldrich, United States of America).

2.2. UV ageing

A subset of the fragments underwent UV irradiation as abiotic ageing process. This type of treatment is the most common to simulate long-term environmental ageing of plastic polymers (Wang et al., 2023). Fragments were put in open glass beakers in air and irradiated from above using UV-B radiation at an intensity of 5 ± 0.4 W/m^2 (as average ± standard deviation after 9 measurements with a Skye SpectroSense2+ system, United Kingdom) in a radiation chamber for 900 h (Xie et al., 2020). This time frame was selected to represent an initial ageing of dispersed plastic in the natural environment, being equivalent to the UV-B radiation dose for about 90 days of natural sunlight in a temperate climate (Pieristè et al., 2019). The content of each glass beaker was mixed and beakers were shifted in position daily to ensure homogenous irradiation of all the specimens and on all the faces of fragments. Changes in surface chemical functional groups were assessed periodically (after 48, 120, 240, 480 and 720 h, respectively) after collecting 2 fragments at each period, while 3 samples were characterized at the end of the experiment (i.e., after 900 h). The samples which underwent this treatment will be labelled as "UV aged" in the following sections.

2.3. Biofouling process

The biofouling process was performed under laboratory conditions. Three algal species were selected to induce biofilm formation. Autotrophs are in fact an important component of the biofilm community found also on environmental plastics (Amaral-Zettler et al., 2020; Di Pippo et al., 2020; Miao et al., 2021; Nava and Leoni, 2021). Three species with distinct traits lineage

were chosen after preliminary testing their ability in participating in biofouling consortia by incubating them with plastic fragments: *Klebsormidium flaccidum*, a filamentous green alga forming colonies up to several millimeters in length (Di Pippo et al., 2020; Li et al., 2022b); *Aphanocapsa muscicola,* a coccoid cyanobacterium with small (<1 μm) and round cells usually forming irregularly shaped colonies, commonly observed on plastic collected from the environment (Shan et al., 2022); and *Botryococcus Braunii,* a green microalga forming floating aggregates already used for environmental ageing studies in mesocosm (Nava et al., 2021). The strains of *Klebsormidium flaccidum, Aphanocapsa muscicola* and *Botryococcus Braunii* are deposited at the NORCCA collection with the internal codification NIVA-CHL 80, NIVA-CYA 474, and NIVA-CHL 145/1, respectively. All algal cultures also contained contamination of unidentified bacterial strain(s).

A preliminary experiment was performed using single-species inocula to test the capacity of biofilm formation on plastic by the different species; since all microalgae showed variable ability of colonizing plastics (see Section 3.3.2), the incubation with a mixed consortium of all the three species was selected to create biofouled fragments. There is no claim this approach produces biofilms closely reflecting those building up in natural settings. However, it was deemed sufficient to provide artificially induced cover of the plastic specimen by a community with relative diversity, that could be useful for the scope of this research.

The biofouling processes were performed in Erlenmeyer flasks pre-washed with detergent and rinsed with ethanol. 150 μl of inoculum of each species from our cultures (inocula were maintained with a density varying between about 100,000 cells/ml for *Aphanocapsa muscicola* and *Botryococcus braunii,* and 1000 cells/ml for *Klebsormidium flaccidum*) were added to 15 ml growth medium in the flasks. The flasks were then placed on an orbital shaker incubator (90 rpm shaking) under continuous visible light radiation (100 μmol/m^2/s of intensity) in the presence of 15 plastic fragments. A biofouling control sample (i.e., growth media and inoculum without plastic) was also analyzed to assess possible differences in algal growth in suspension induced by plastic (such as plastic-induced toxicity). The biofouling build-up was continued for 10 days. Four plastic fragments per flask were collected after 1, 5 and 10 days of incubation to analyze the growth of algal biofilm and the surface physicochemical properties. The specimens used for metal sorption experiments were transferred directly in the bottles (see Section 2.6).

The biofouling process (as described in this section) was performed both on pristine and previously UV aged specimens. Pristine specimens after biofouling will be labelled as "biofouled" samples in the following sections, while previously UV aged specimens will be labelled as "UV aged – biofouled".

2.4. Quantification of algae in biofilm and suspension

Collected fragments were rinsed twice in deionized water to remove non-attached biological material and left 24 h in air to dry. After drying, the plastic fragments were placed in a 24 well plate (1 fragment per well, using 4 replicates for each incubation batch). Then, two distinct methods were used to determine biofilm growth: i) fluorescence analysis of chlorophyll and ii) optical microscopy method to measure coverage rates of plastic fragments. We analyzed chlorophyll fluorescence directly on plastic fragments: fluorescence was measured at 685 nm using the exciting wavelength at 485 nm (Li et al., 2022b) by means of a Spectramax iD3 (Molecular Devices, United States of America) plate reader. We applied a well scan mode with 32 measures equally distributed on the well surface and we then calculated an average value of fluorescence for every fragment. Plastic fragments without biofilm were used as sample blanks. We then analyzed the same plastic samples through optical microscopy to measure the percentage of total plastic surface covered by biofilm. For this, stereomicroscope images of plastic specimens were captured using a Nikon SMZ 745T stereomicroscope with Infinity 1-3C camera and Infinity Analyze software. Images were processed using ImageJ software plugged into the colseg color segmentation plugin (Loo et al., 2012). This enabled a direct measure of the covered area.

In addition to these measurements, the algal densities in suspension were measured at 0, 1, 5 and 10 days of experiment to ensure similar biomass growth in all incubation batches. Fluorescence measurements were used to this scope (Li et al., 2022b) through analyzing aliquots of 0.5 ml of the cultures in a 24-well plate using a Spectramax iD3 (Molecular Devices, United States of America) plate reader for chlorophyll fluorescence, using the same method described above.

2.5. Physicochemical characterization of plastic samples

Plastic characterization included Fourier-transformed infrared (FTIR spectroscopy) analysis, scanning electron microscopy (SEM) and water contact angle measurement. These analyses were performed on pristine, UV aged (after 900 h), biofouled (after 10 days of incubation) and UV aged - biofouled specimens. Samples were analyzed for surface properties selecting a random side of the larger face of the fragment, since the analysis of different areas of the surface yielded a variance comparable to the analysis of different fragments. In addition, metal content in pristine plastics was assessed by an acid digestion protocol.

Surface functional groups were analyzed using a Frontier FTIR (Perkin Elmer, United States of America) equipped with a diamond crystal accessory for collection in attenuated total reflection mode. 12 scans were performed for each measurement, taken in the 4000–650 cm^{-1} wavenumber window at a spectral resolution of 4 cm^{-1}. A background measurement was taken before each individual specimen was analyzed. FTIR data processing was performed using Spectragryph software v1.2.15. Infrared spectral data were scaled (from 0 to 1) on the maximum absorbance peak and smoothed using the Savitzky–Golay filter (applying a window of 25 points and a polynomial order of 3). Baseline was also corrected through an adaptive baseline algorithm (50 % of coarseness). Different indexes were then obtained to quantitatively compare the alteration of specific bands by abiotic ageing and biofouling (Eq. (1)):

$$Index_b = \frac{A_b}{A_{ref}} \tag{1}$$

where *Index$_b$* is the index of the specific FTIR band analyzed: carbonyl group (1715 cm^{-1}); hydroxyl group (3300 cm^{-1}); amide I (1650 cm^{-1}) and II (1550 cm^{-1}); and polysaccharides (1040 cm^{-1}); A_b is the absorbance value obtained at the wavelength of a specific functional group, and A_{ref} represents the absorbance values at the reference bands (Binda et al., 2023a, 2023b). The following reference bands were selected for the different plastic polymers: the CH$_2$ peak at 1465 cm^{-1} for PE (Martínez et al., 2021), the CH$_2$ bend peak at 1455 cm^{-1} for PP (Jung et al., 2018) and the reference peak at 1452 cm^{-1} for PLA (Palai et al., 2021; Palsikowski et al., 2018).

The micromorphology of surface features was investigated through a Philips® (Netherlands) field emission gun SEM, with a 25 keV beam under high vacuum conditions. Samples for SEM were covered with a ~5 nm thick and uniform gold layer using a Cressington (United Kingdom) 108 auto vacuum sputter coater to improve image quality.

Hydrophobicity (or hydrophilicity) of plastic specimens was analyzed by water contact angle measurements using the sessile drop method. Approximately 2 μl of distilled water was dropped on the surface of the plastic sample through a syringe using a drop shape analyzer (OCA-20, Dataphysics, Germany). Then, the contact angles were computed through ellipse fitting using SCA20 software (Dataphysics, Germany).

Acid digestion of pristine plastic specimens was performed to analyze the total content of metals in plastic samples. The inorganic compounds present in the plastic matrix may in fact affect the results of sorption experiments (Hildebrandt et al., 2021). Briefly, about 60 mg of plastic fragments were weighed and inserted into a Teflon vessel. 4 ml of nitric acid 65 wt% were added. The samples were then digested in a ETHOS One Milestone (United States of America) microwave at 180 °C for 25 min. The digested solution was cooled and diluted in ultrapure water. Potential solid residual in the solution was removed by filtration with cellulose filters (0.45 μm

pore diameter) and solution was analyzed using a Thermo Scientific Icap-Q ICP-MS (United States of America) for 12 different metals (sodium, Na; magnesium, Mg; Al, potassium, K; titanium, Ti; chromium, Cr; manganese, Mn; iron, Fe; nickel, Ni; Cu; zinc, Zn; barium, Ba). These analyses were performed in University of Insubria (Italy) laboratories. Further experimental details are available elsewhere (Binda et al., 2023a).

2.6. Metal sorption experiments

Pristine and aged fragments (with the three different treatments) were tested for sorption of Al and Cu ions in solution. First, all plastic fragments were rinsed with distilled water before being transferred to the solution containing the metals. Solutions were spiked with Al and Cu (using the stock solutions described in Section 2.1) to reach final concentrations of 1.00 ± 0.06 mg/l (as average $\pm$ standard deviation, after 3 replicates). These concentrations represent expected values in polluted water bodies, but are also representative for natural occurring concentrations in areas with high geochemical background values (Binda et al., 2020; Nordstrom, 2015). A $NaNO_3$ buffer (reaching the final concentration of 0.01 M) was added in solution to adjust ionic strength and pH was corrected to 6.0 ± 0.1 (as average $\pm$ standard deviation, after 3 replicates) using 0.01 M NaOH and 0.01 M HNO_3 solutions and a Dupla (Germany) pH electrode (Qiongjie et al., 2022).

Sorption kinetics was first assessed to observe the time required to reach equilibrium in sorption batches at 1, 6, 18, 24, 48 and 72 h time intervals. For each batch, 15 plastic fragments were added in 15 ml of buffered metal containing solution. The bottles were closed and put in an incubator with orbital shaker at 100 rpm and room temperature (20 °C).

The sorption experiments were performed in 30 ml PP bottles, previously rinsed with 2 % (v/v) HNO_3 for 24 h and conditioned with the same solution used for experiment for 48 h (Sanvito and Monticelli, 2021), then rinsed with ultrapure water. Any potential adsorption to the walls of the bottles was calculated by measuring the reduction in dissolved metal concentrations in procedural blanks (i.e., bottles with the metal solution, but without any plastic fragments). Potential release of metals from the plastic fragments themselves (e.g., from metal-containing additives; Turner and Filella, 2021) or from the biofilm on the fragments was assessed by exposing 15 plastic fragments of every polymer and ageing type in separate bottles to 0.01 M $NaNO_3$ solutions without any metals (control samples). All sorption experiments were performed with 3 replicates of each batch. At every time interval (for kinetics assessment) and the end of each sorption experiment, 0.2 ml of solution was collected and filtered on cellulose filters (0.45 μm pore diameter), diluted with ultrapure water, acidified with Suprapur HNO_3 to reach 2 % in volume and analyzed for Cu and Al by an Agilent 7700 ICP-MS (United States of America). These measurements were performed at the Norwegian Institute for Water Research laboratories (Norway), following EN ISO 17294-1:2007 and EN ISO 17294-2:2016 standard operating procedures. At the end of experiment, in addition, plastic fragments were separated from the solution, air dried for 24 h and weighed (weights are listed in Table S1).

The per cent loss (depletion, Eq. (2)) of Al and Cu from the solution over the exposure period was calculated from the difference in the initial concentration (C_0, mg/l) and the concentration at equilibrium (C_e, mg/l), taking into account correction caused by any releases from plastic fragments and biofilm (C_r, mg/l):

$$depletion\ (\%) = \frac{(C_0 + C_r - C_e)}{C_0} \times 100 \tag{2}$$

This value was calculated for the procedural blanks and the samples with plastic. A depletion value for Al or Cu higher than the procedural blank indicates a concomitant sorption of Al or Cu to the plastic fragments. Depletion was therefore used as proxy of sorption capacity. While this simplified approach does not permit a complete mass balance in the sorption batches (e.g., Hildebrandt et al., 2021), it yields sufficient information to compare the depletion of dissolved (and potentially bioavailable) metals

with different plastic type and ageing processes, taking also into account both the metal release from plastic specimens and the adsorption by the bottles used for experiments.

Sorption capacity (q, μg/g) was also calculated as follows (Eq. (3)) to model sorption kinetics:

$$q = \frac{(C_0 + C_r - C_e) \times V}{m} \tag{3}$$

where m (g) is the weight of plastic fragments added and V (l) is volume of the solution. The pseudo-first order and pseudo-second order equation were then used to model sorption kinetics (Eqs. (4) and (5), respectively):

$$\ln (q_e - q_t) = \ln q_e - k_1 t \tag{4}$$

$$\frac{t}{q_t} = \frac{1}{k_2 q_e^2} + \frac{t}{q_e} \tag{5}$$

where and q_e (μg/g) q_t (μg/g) are the sorption capacity value at equilibrium and at specific time t (min); k_1 (1/min) and k_2 (g/μg × min) are the rate constants for pseudo-first order and the pseudo-second order, respectively (Binda et al., 2022; Rozman et al., 2023; Tang et al., 2020).

2.7. Statistical analysis

All datasets were evaluated for normality using a Shapiro-Wilk test prior to further analysis. Since data on FTIR spectra indexes and contact angles all showed normal distributions, a one-way ANOVA with Tukey post-hoc test was performed on these data to validate differences between pristine and aged (by UV irradiation and biofouling) plastic fragments. The non-parametric Kruskal-Wallis ANOVA was used to validate differences in depletion rates of Al and Cu among ageing processes (i.e., UV ageing and biofouling) as well as among different polymers, since assumptions of normality and homogeneity of variance were violated. This non-parametric test was also used to assess the factors affecting biofilm cover on different plastic polymers. Statistical tests were performed using Origin 2018 software (OriginLab Corporation, 2018).

3. Results and discussion

3.1. Changes in physicochemical properties after ageing processes

UV ageing affected the abundances of carbonyl and hydroxyl groups on the surface of both PE and PP plastic. We observed significant increases in the FTIR carbonyl and hydroxyl indexes on these polymers with increasing UV irradiation time. This is assumed to be caused by polymer oxidation as reported by others (Ainali et al., 2021; Campanale et al., 2023; Liu et al., 2021c; Martínez et al., 2021). On average, a threefold increase in the FTIR carbonyl index was observed for PE, while the hydroxyl index was somewhat less pronounced for PE (by a factor of 1.5); PP showed instead a more than tenfold increase for both the indexes after UV ageing (Fig. 1a-b). Apparently, the PLA fragments were less affected by UV ageing than the PE and PP fragments, as indicated by more scattered changes in the carbonyl and hydroxyl indexes (Fig. 1 and Fig. S1).

The formation of a biofilm on the plastic fragments resulted in an increase in amides and polysaccharides signals (all showing an at least twofold increase compared to pristine and UV aged samples) but not the carbonyl signal, on the FTIR spectra (Fig. 1 and Table S1). Only a few exceptions were observed: UV aged - biofouled PP specimens showed a distinct trend. These fragments had lower biofouling coverage than all the other analyzed specimens (see Section 3.3.2). Biofouling also yielded an increase in hydroxyl groups on the surface of plastics with index values twice as after UV ageing, confirming previous results (Binda et al., 2023b). Again, this effect was not observed in UV aged - biofouled PP samples. Carbonyl formation appeared to be more associated with UV ageing than biofouling. Interestingly, the biofouling on plastics previously aged with UV resulted
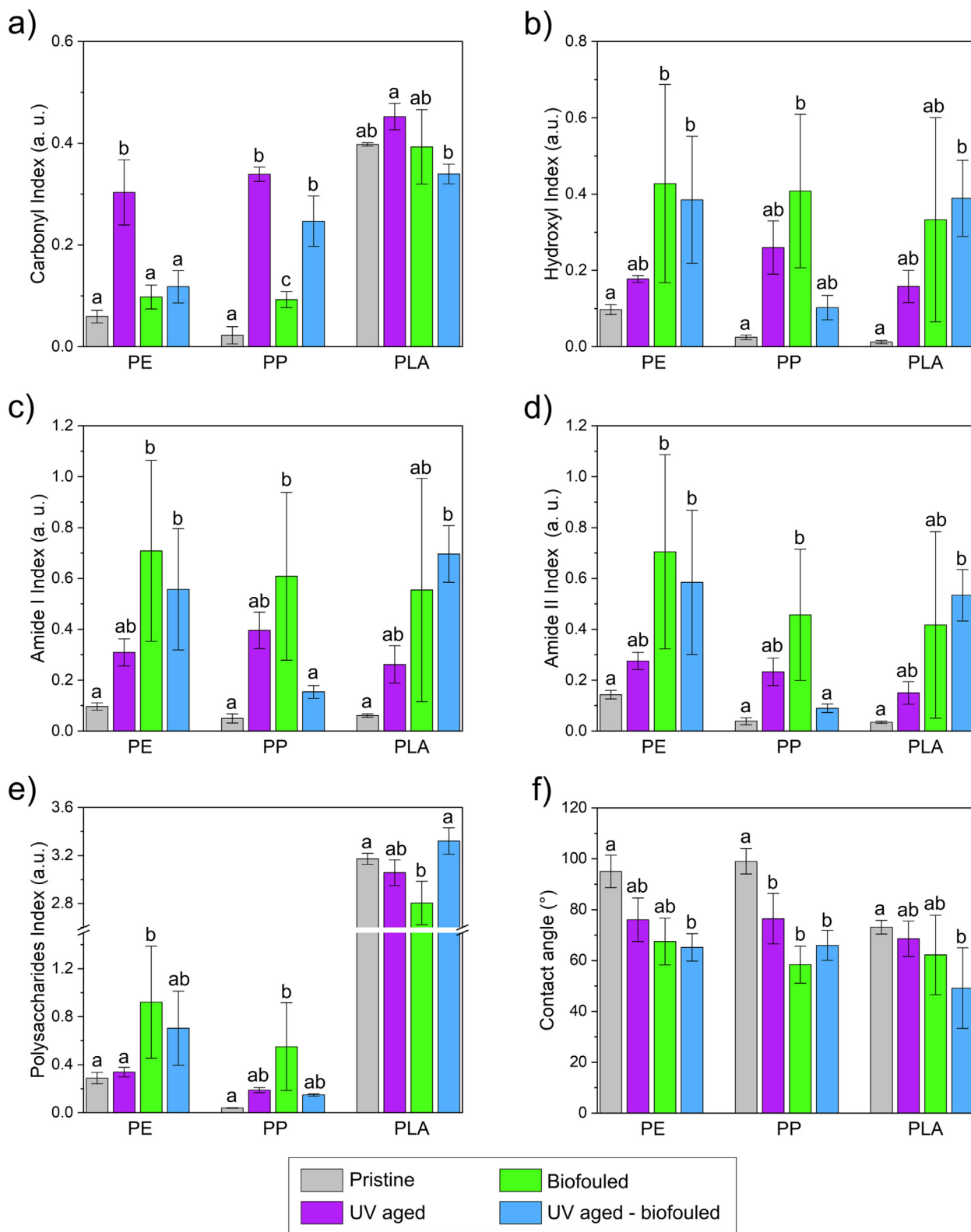
Fig. 1. FTIR bands indexes (a, b, c, d, e) and contact angle measurements (f), expressed as average ± standard deviation after 3 replicates. Different letters indicate significant different measurements by one-way ANOVA and Tukey tests.

in "masking" the UV-induced increase in the carbonyl index, especially for PP and PE. The functional groups' profiles of the samples treated with this combined abiotic and biotic ageing processes tended not to be significantly different from the one of the samples only treated with biofouling (see, as an example, the PE indexes in Fig. 1a-d). This is also observable from the

changes in the carbonyl index at different incubation times: as an example, the carbonyl index of previously UV aged PP ($p = 0.04$) and PE ($p = 0.01$) reduced at increasing incubation time, while this value increases ($p = 0.038$ for PE and $p = 0.03$ for PP) at increasing incubation time for pristine polymers (Table S1). This can be easily interpreted as a "cover" effect,

whereby the outer eco-corona prevalently determines the characteristics of the plastics surface.

The characterization of surface functional groups is a useful endpoint to assess possible changes in chemical and physical properties that can contribute to increased affinity for binding polar substances such as metals. However, this assessment should consider all the confounding factors. For instance, in some cases, functional group indexes can be affected by spectral interferences; this applies especially to oxygen-containing polymers. In PLA samples, the carbonyl index was affected by the polymeric composition rich in carbonyl groups. Similarly, the polysaccharide index overlapped with the bands of primary, secondary, and tertiary hydroxyls (Zheng et al., 2023). Despite these confounding factors, our analysis indicates that all types of ageing tend to increase the presence of polar or charged groups on the polymer surface, which can alter both the hydrophobicity of the surface and the affinity for charged species in the solution, increasing the likelihood at least for a different type of non-covalent bonds.

The changes in wettability induced by ageing are presented in Fig. 1f. As expected, the increase in oxidized groups due to UV ageing coincided with a change in hydrophobicity. Polyethylene and PP showed a significant decrease in water contact angle after any type of ageing process: while the pristine PP and PE presents a substantially hydrophobic surface, the UV ageing process yield an average decrease of water contact angle by 10°. This effect was less evident in PLA, possibly due to this polymer already having a more hydrophilic surface in the pristine form compared to PP and PE and displaying a less evident change after UV irradiation. Biofouling

further decreased the water contact angle value for all polymers, both pristine and previously UV aged. Similar observations were made in earlier studies (Binda et al., 2023b; Pete et al., 2023).

SEM analysis revealed several changes in surface micromorphology following UV ageing of the plastic polymers (Fig. 2). The polymers were diversely affected by UV ageing: PP showed the strongest effect presenting wide cracks (few mm long) in several surface sites following irradiation. We also noticed evenly distributed microcracks (a few hundred nanometer long) broadly distributed on the whole surface of PP. This polymer is known to be more brittle than others commonly used polymers such as PE (Reineccius et al., 2022). The breaking of polymer chains induces this fragility due to oxidation and the formation of free radicals that propagate the reaction across the surface and inside the polymer matrix. These molecular processes propagate forming nano and microcracking (Duan et al., 2022). The surface micromorphology of PLA showed a pattern similar to PP with diffuse microcracks (<500 nm long), but with less marked changes than PP. Polyethylene instead showed a substantially higher resistance to UV ageing. While the surface of PE also appeared to become rougher, the number and dimension of microfractures was much smaller compared that of the other polymers analyzed here.

The results of surface morphological characterization following UV irradiation observed here are partially discordant with previous reports, specifically for PLA (Fan et al., 2021). This may be related to the different processes and time frame of the ageing adopted in the different studies. Also, the physical, chemical and morphological features of the materials
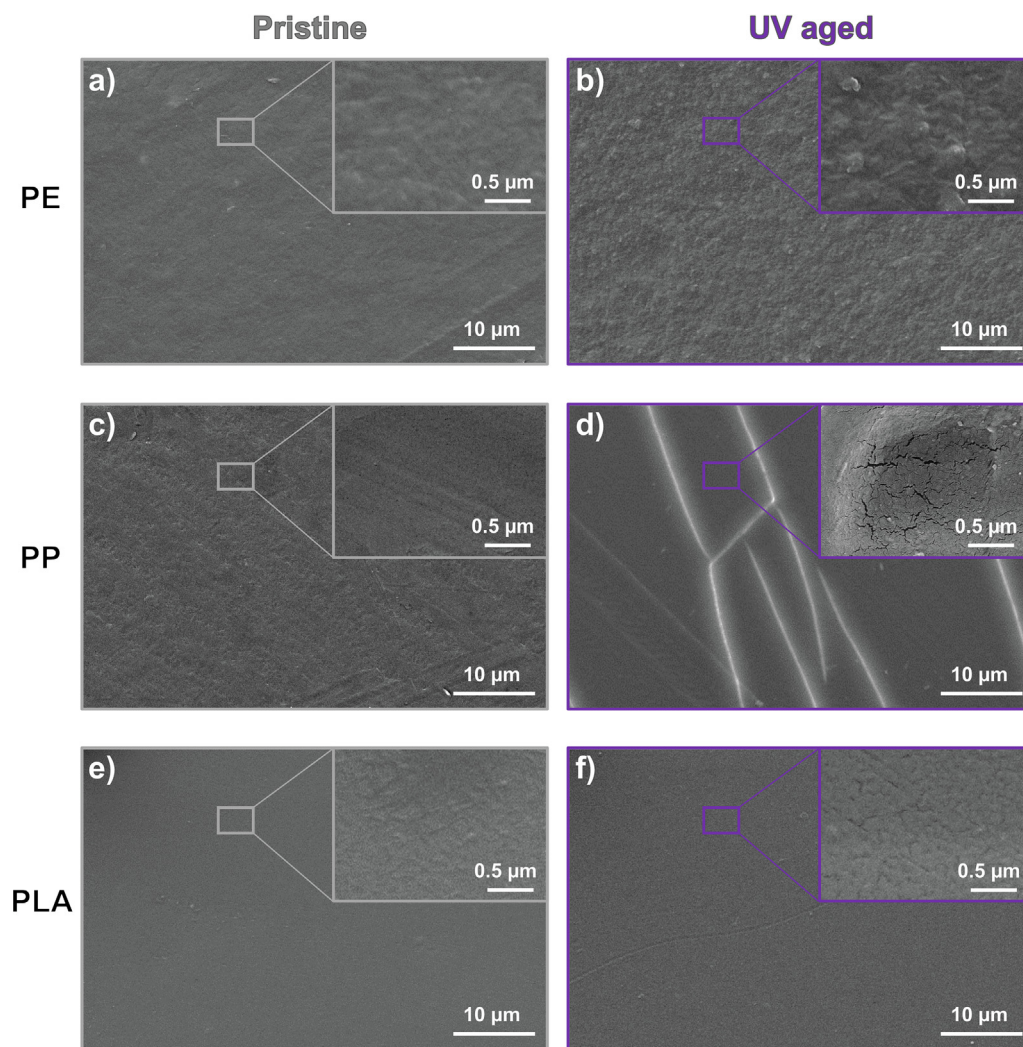

Fig. 2. SEM micrographs of pristine (a, c, e) and UV aged (b, d, f) plastic fragments at 2000× magnifications. The insets show details at 32,000× magnifications.

selected in this study may play a role: we obtained plastic samples from commercial items (extruded films), which are likely to contain a suit of chemical additives to give desired properties for the designated uses of the final product. These additives may play a major role in determining the resistance of plastics to UV ageing (Langford et al., 2015). However, this factor is rarely characterized or addressed in this type of study, since previous research utilized virgin plastic pellets (Duan et al., 2022; Fan et al., 2021; Zvekic et al., 2022). Virgin pellets possibly involve a simplified mixture of chemical additives, likely lacking the set of UV protection additives that are typically added during conversion, limiting their representativeness for studies focusing on environmental processes. Other factors may also be involved in defining the ageing trends observed in this study, such as plastic crystallinity, which is altered during plastic production process (Ainali et al., 2021; Herath and Salehi, 2022). We therefore suggest future studies to compare the role of polymer physicochemical properties and additive content in defining plastic abiotic ageing.

The SEM micrographs of biofouled plastics clearly showed the formation of the algal biofilm on plastic surface (Fig. 3). We observed filaments of *Klebsormidium flaccidum* up to a few millimeters long, aggregate colonies of *Botryococcus braunii* and smaller aggregates of *Aphanocapsa muscicola* in all the specimens, regardless of the previous ageing treatment. In some cases, we observed the consortium of the three species covering the same area (such as in Fig. 3b-c). This indicates that colonization by algae happened in all types of polymers used in this experiment and is likely also occur in environmental settings. However, the quantity of surface covered by biofilms was variable among the different plastic samples, as well as before and after the UV ageing process (these differences are described in detail in Section 3.3.2).

Interestingly, PLA samples showed a mechanically degraded surface emerging after the development of the biofilm (especially with *Klebsormidium*

flaccidum). This effect can be linked to the degradability of this polymer which can both be driven by hydrolysis and biodegradation (Chia et al., 2020). While it is obviously not expected that algae utilize PLA as a carbon source, colonization by algae could add mechanical stress that speed up degradation by hydrolysis or by heterotrophs microorganisms. Some algal exudates, for example, have been pointed out as a promoter for hydrolysis of biodegradable polymers (Chia et al., 2020; Nava and Leoni, 2021).

3.2. Sorption of metals and comparison of ageing processes

Metal sorption process reached an equilibrium after 48 h (Fig. S2). Concerning the behavior of sorption kinetics (model parameters are listed in Table S2), the pseudo-first order kinetics model well described the sorption process of Cu on most pristine and UV aged polymers, except for pristine PLA. This model also well described the sorption process of Al onto pristine PLA, pristine PP and UV aged PP. In the case of pristine and UV aged PP Cu depletion was instead not statistically different from blanks, indicating that sorption was negligible. All the biofouled and UV aged-biofouled polymers showed an sorption process better described by pseudo-second order model compared with the pseudo-first order, in accordance with previous research (Chen et al., 2022; Guan et al., 2020; Qiongjie et al., 2022). This indicates that biofouled plastic likely sorb metals through a different process compared to pristine and UV aged ones. Control samples including only the metal solution (without plastic specimens) showed that the pristine PP bottles used for the experiments did not measurably affect the dissolved concentrations of the metals (Table S3). Similarly, as shown in Table S4, the release of metal contained in the polymer matrix is close (or below) the detection limits in most of the pristine and UV aged samples. A limited amount of these metals was released from biofouled plastics and was used to correct depletion and sorption capacity values (see Section 2.6).
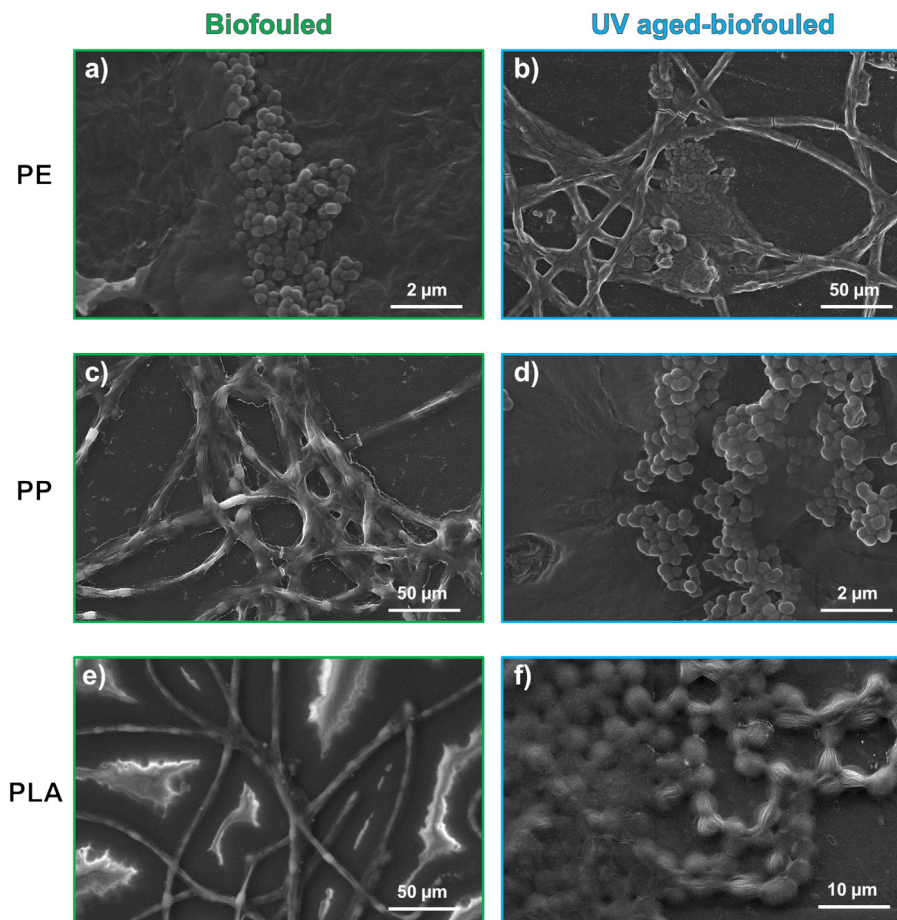

Fig. 3. SEM micrographs of biofouled fragments in all polymer samples, both pristine (a, c, e) and previously UV aged (b, d, f) at different magnifications.

The depletion values for Al and Cu measured at the kinetic equilibrium and aggregated for the different treatments are shown in Fig. 4. All the pristine polymers affected the initial concentration of Al and Cu only to a limited extent, while UV ageing possibly increased the sorption of Al, especially in PE (Table S3). This different behavior of PE is at the origin of the skewed distribution for the UV treatment in Fig. 4. Cu sorption was instead not affected by UV ageing. In contrast, a significant ($p < 0.05$) change in the depletion value of both metals was observed following biofouling, both for pristine and previously UV aged polymers. Biofouled plastic, in fact, sorbed up to 35 % of the Cu and 25 % of Al in the water solution.

In light of these results, we tested the significance of the depletion results in relation to different treatment types: the main premise of this study is that biofouling mainly influences the sorption of metals on plastic. Results in Table 1 showed that the statistically significant factors affecting the differences in dissolved Al and Cu depletion are the biofouling itself or in combination with UV ageing, confirming the hypothesis. Biofouling had a stronger effect on metal depletion in water (highlighted by a higher Chi squared value) than its combination with UV ageing. This reinforces the understanding that the eco-corona on environmental plastics governs the sorption and exchange of metals with the surrounding environment. Other studies already reported increased sorption rates of metals after biofouling in plastic (Guan et al., 2020; Li et al., 2022a; Liu et al., 2021b; Liu et al., 2021a; Stabnikova et al., 2022), but to the best of our knowledge, the central role of this process had never been addressed systematically.

3.3. Assessing the key role of biotic ageing in metal sorption

The results presented in Fig. 4 highlighted that biofilm formation is the key process for the sorption of metal ions from the solution, regardless of the polymer type and the previous abiotic ageing. These results highlighted that while different plastic polymers inherently have limited affinity toward metal sorption in water owing to their hydrophobicity, this material represents a suitable substrate for biofilms which accumulate metals from the surrounding water environment. While here we used Cu and Al as examples, it is likely that other metals (especially essential ones) behave similarly. In light of this understanding, environmental plastic should be considered a new type of habitat hosting a community that is involved in resource exchange with other parts of the ecosystems. Therefore, we looked more in detail at the efficiency of this sorption by characterizing it at varying biofilm coverage levels in the different polymer types and the previous ageing processes.
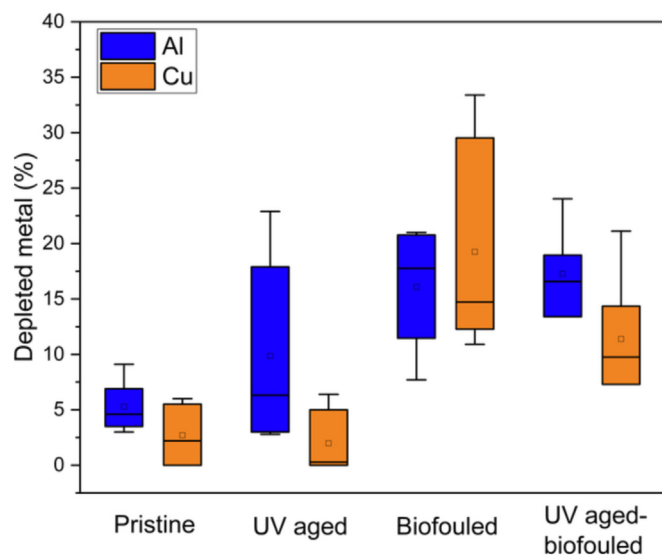
Table 1

Chi squared and *p* values output of Kruskal-Wallis ANOVA for Cu and Al depletion in sorption experiments. The tested factors are the polymer type, UV ageing, biofouling and the combination of both ageing processes. Significant values ($p < 0.05$) are listed in italics.

Factor	Al		Cu	
	Chi squared	*p* Value	Chi squared	*p* Value
Polymer type	4.61	0.10	2.77	0.25
UV ageing	1.03	0.31	0.60	0.44
Biofouling	*15.14*	*<0.0001*	*26.39*	*<0.00001*
UV ageing - biofouling	*6.63*	*0.012*	*4.*	*0.039*

3.3.1. Sorption capacities at different incubation times

The dependence of metal sorption on the level of biofilm coverage was assessed using linear regression. For this, we first plotted the mean values of depletion (of Al or Cu from the dissolved phase) calculated across all type of polymers and previous UV ageing process against the time lapsed from the addition of the algal inoculum (Fig. 5a-b). For most of the polymers, regardless of previous ageing process, the incubation time for biofouling prior to the sorption experiment is positively correlated with the sorption of metals. This trend is more evident for Cu.

Next, we directly plotted the mean depletion values against the mean percentage of biofilm coverage (Fig. 5c-d). A positive ($p < 1 \times 10^{-6}$, $R^2 > 0.7$) correlation was observed between algae coverage and adsorbed Cu from the solution. The same trend was also observed for Al ($p = 0.005$); however, depletion data of Al were more scattered, especially in the lower range of biofilm cover % ($R^2 = 0.299$). Three main features can explain these differences in sorption behavior between the two metals: i) the anomalous trend of PE samples showing substantial Al depletion from the dissolved phase even without biofilms, ii) the different chemical speciation of these metals, and iii) the different interaction mechanisms of algae with Al and Cu (Botté et al., 2022; Gundersen and Steinnes, 2003).

In more detail, considering the first feature, in Fig. S2a and Table S3 a notable affinity of PE (especially after UV ageing) for Al is observable, whereas this trend was not evident for Cu. This effect was also evident in the outputs of the Kruskal-Wallis ANOVA test (Table 1): the polymer type showed a tendency to be correlated with Al depletion, while being still not statistically significant ($p = 0.1$). The apparently higher affinity of PE fragments to metals can potentially be explained by the presence of organic and inorganic additives (such as UV quenchers, fillers, pigments and plasticizers) which can be released at the solution interface after UV ageing, possibly complexing or forming insoluble salts with Al and reducing its concentration in the dissolved phase. PE fragments presented in fact the highest content of some of the metals analyzed (i.e., Mg, K, Zn and Ba, Table S5): these elements, likely present in the polymer matrix as oxides and salts (Turner and Filella, 2021), can be involved in Al precipitation at the experimental conditions used in this study. Inorganic fillers, in fact, have been already observed to alter metal sorption processes on plastic (Zhou et al., 2022). The leaching of polymer additives, however, did not alter the solubility equilibrium of Al: pH in the batches did not show changes after sorption experiments (Table S6).

The different depletion of Al and Cu can also be explained by their chemical speciation in water (feature ii): Al is, in fact, more likely to form insoluble hydroxides and colloids at almost neutral pH, which can possibly coprecipitate on plastic or biofilm surface: at slightly acidic pH, in fact, the most abundant species is $Al(OH)_2^+$, presenting low solubility in water (Botté et al., 2022; Johan et al., 2021); Cu is instead present as Cu^{2+} in these conditions, leading to adsorption through complexation on the biofilm surface or by active absorption in the cells of algae (Gundersen and Steinnes, 2003; Ndungu, 2012; Plöger et al., 2005).

Another process possibly affecting the observed differences in Al and Cu depletion is related to the different role of these metals in the physiology of the microorganisms forming the biofilms (feature iii): Cu is, in fact, an essential element which can be actively transported into the algal cells, while Al is a non-essential element which is more likely to be passively
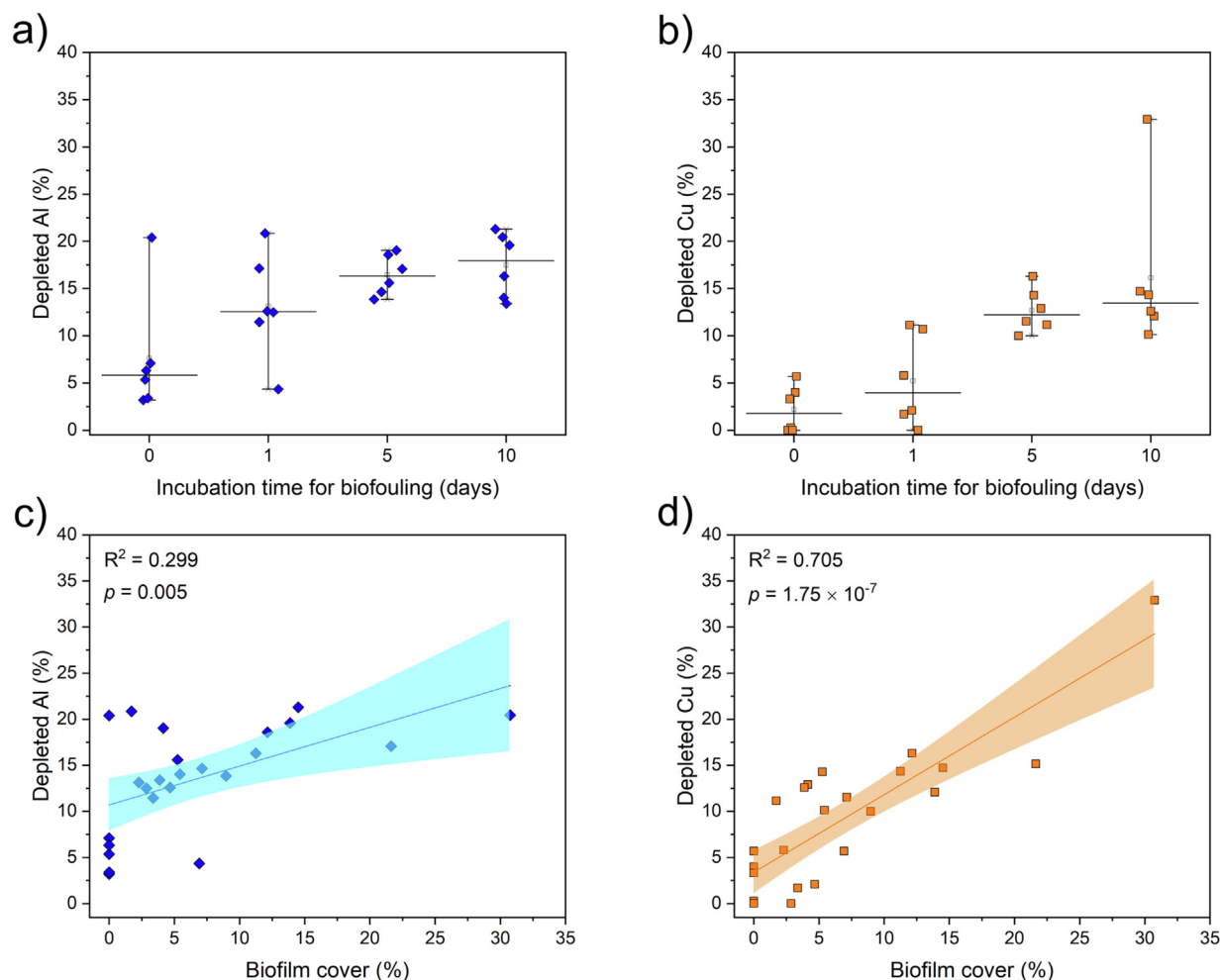

Fig. 4. Box and whisker plot showing depleted Al (blue) and Cu (orange) in all sorption experiments.

Fig. 5. a-b) Average Al (a) and Cu (b) depletion from the dissolved phase at different incubation times (times are measured from the addition of the algal inoculum). c-d) Linear correlation between Al (c) and Cu (d) depletion from the dissolved phase and the level of biofilm coverage. The plots include data for all types of polymers.

adsorbed in the extracellular matrix (Worms et al., 2006). This can cause a less evident correlation of Al with the biofilm coverage, while still biofouling show a significant increase in its sorption on plastic fragments (Table 1 and Fig. 5). Although the main aim of the study was to investigate the plastic-related processes in affecting metal sorption, the observed differences between Al and Cu highlight that also the chemical properties of metals determine their interactions with this substrate (Binda et al., 2021).

3.3.2. The role of plastic as a substrate for biofilm colonization

This study highlighted the key role of biofilm formation on plastics in determining exchanges of metals and nutrients with the surrounding water. Hence, it is important to also assess the role of plastic properties in defining colonization rate and assemblage of the eco-corona (Nava and Leoni, 2021). The inherent properties of different types of plastic substrate have been already documented to affect biofilm establishment and growth, especially in the pioneering community at the early stage of the eco-corona formation (Djaoudi et al., 2022; Ramsperger et al., 2020; Tong et al., 2021). Similarly, the physiological features of organisms composing the biofilm and the surrounding conditions can affect this process (Ganesan et al., 2022). In this study we focused especially on the factors affecting biofouling rates considering the plastic and the analyzed species forming biofilms.

The biofilm growth yielded variable coverages of the different plastic specimens analyzed (Fig. 6). As for other biological substrates, the plastic surface plays a role in defining cell attachment and following biofilm growth. Here UV ageing negatively affected the coverage by algae, while the polymer type only did not significantly affect biofilm growth (Table 2). The negative effect of UV ageing on the biofouling process can be explained

by the changes in hydrophobicity (observed in Fig. 1f): hydrophobic substrates (pristine PE and PP, with water contact angle >90°), in fact, presented a significantly higher coverage of algae after 10 days of experiment (Fig. 6 and Table 2). This agrees with other studies on microalgal biofilms (Tong et al., 2021). Another factor (not addressed in this study) that can affect biofouling rates after UV ageing is the release of chemical additives from the polymer matrix, which may induce toxicological effects. Leaching of chemical additives is often linked to embrittlement of plastic surface and fragmentation which, in turn, results from ageing (Luo et al., 2022).

Expectedly, there was a general high variance in coverage rates among different plastic specimens even when they belong to the same batch (Fig. 6) and the algal growth in the dissolved phase of different batches was similar (with a relative standard deviation below 20 %, Fig. S3a). The initial formation of biofilm is driven to a certain degree by random processes that determine the success of the attachment of the microorganisms on the plastic surface (Nava and Leoni, 2021; Shan et al., 2022; Tong et al., 2021; Yu et al., 2023). This was also evident from the results of preliminary incubation experiments testing the ability of algae to form biofilms on plastic (see Section 2.3). We also observed differences in the way the algae species colonized the plastic fragments: the three species displayed different attachment and biofilm growth on plastic fragments when incubated separately, compared to the overall coverage when incubated in mixture, confirming that algal physiology and interspecific interactions affect biofilm formation, too (Table S7).

As a final note, the two methodologies used to assess biofilm cover (i.e., the microscopic analysis and chlorophyll fluorescence measurements, see Section 2.4) were well in accordance (Fig. S3b). Biofilm coverage in
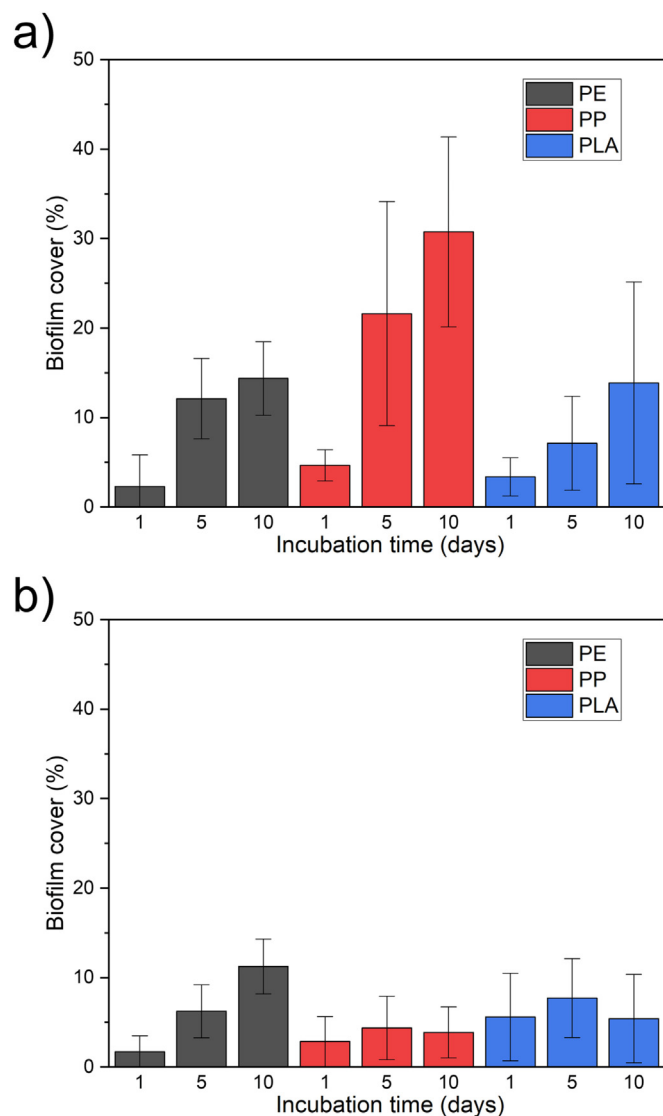
Fig. 6. Biofilm cover (% of surface) for the analyzed polymers at 1, 5 and 10 days of incubation. Panel a) shows the coverage of pristine polymers, while panel b) of UV aged polymers.

percentage was selected for the description in this paper for the sake of simplicity.

4. Conclusions

In summary, this study aimed at disentangling different ageing processes (abiotic and biotic) of environmental plastic and the implications for the sorption of metals through a factor-based study. The selected factors

Table 2
Chi squared and *p* values of Kruskal-Wallis ANOVA for algal coverage after 10 days of incubation. The tested factors are the polymer type (PE, PP and PLA), UV ageing (pristine and UV aged polymers) and surface hydrophobicity (categorized as hydrophobic, with water contact angle >90°; or hydrophilic, with water contact angle <90°). Significant values ($p < 0.05$) are listed in italics.

Factor	Biofilm cover	
	Chi squared	*p* value
Polymer type	1.88	0.39
UV ageing	*7.26*	*0.007*
Hydrophobicity	*8.44*	*0.0037*

were i) the polymer type; ii) abiotic ageing through UV-induced oxidation, iii) biotic ageing using algae, and iv) a combination of both ageing processes. All of these factors were shown to jointly affect plastic properties: the polymer type defines surface functional groups and wettability, whereas both UV ageing and biofouling led to increased wettability of plastic surfaces and induced several changes in surface functional groups and micromorphology. These results further support the importance of considering plastic ageing processes to increase the environmental relevance of the studied effects (Rozman and Kalčíková, 2022). Our results show that biofouling represents the most effective factor in defining the metal sorption from aqueous solutions. Biofilm formation had already been identified as an important component of plastic ageing (Stabnikova et al., 2022), but this study permitted to statistically test the relevance of this factor in governing metal sorption under controlled conditions and with a factorial design. In addition, the chemical properties of the metal affected its sorption to plastic surfaces, since differences were observed between the two metals analyzed in this study (Al and Cu). The findings of this study indicate that pristine plastic can limitedly act as a potential scavenger of metals in water. Instead, based on our findings, we suggest to further investigate the analysis of plastic as a specific substrate for a distinct microbiological community, and the broader evaluation of biofouling on the ecological implications for micronutrient availability. This exploration can open a new venue in plastic environmental research: the metal depletion induced by biofouled plastic in this study can have potential environmental implications, such as the sequestration potentially toxic metals in biofilm and the competition for essential (micro)nutrients with the natural planktonic community. Subsequent experimental studies should assess the environmental relevance of these processes.

CRediT authorship contribution statement

Gilberto Binda: funding acquisition, methodology, investigation, writing – original draft; **Margarida Costa**: methodology, writing – review and editing; **Luka Supraha**: methodology, investigation; **Davide Spanu**: investigation, data curation; **Christian Vogelsang**: resources, writing – review and editing; **Eva Leu**: methodology, writing – review and editing; **Luca Nizzetto**: funding acquisition, conceptualization, supervision, writing – review and editing.

Data availability

Data are available as supplementary material and at the following link: https://doi.org/10.5281/zenodo.7920327

Declaration of competing interest

The authors declare that they have no known competing financial interests or personal relationships that could have appeared to influence the work reported in this paper.

Appendix A. Supplementary data

Supplementary materials including supplementary Figs. S1-S3 and Supplementary Tables S1-S7 can be found at the web version of this article. Original data of FTIR spectra are instead available at the following online dataset, DOI: https://doi.org/10.5281/zenodo.7920327.

References

Ainali, N.M., Bikiaris, D.N., Lambropoulou, D.A., 2021. Aging effects on low- and high-density polyethylene, polypropylene and polystyrene under UV irradiation: an insight into decomposition mechanism by Py-GC/MS for microplastic analysis. J. Anal. Appl. Pyrolysis 158. https://doi.org/10.1016/j.jaap.2021.105207.

Amaral-Zettler, L.A., Zettler, E.R., Mincer, T.J., 2020. Ecology of the plastisphere. Nat. Rev. Microbiol. 18, 139–151. https://doi.org/10.1038/s41579-019-0308-0.

Bellasi, A., Binda, G., Pozzi, A., Galafassi, S., Volta, P., Bettinetti, R., 2020. Microplastic contamination in freshwater environments: a review, focusing on interactions with sediments and benthic organisms. Environments 7, 30. https://doi.org/10.3390/environments7040030.

Bellasi, A., Binda, G., Boldrocchi, G., Pozzi, A., Bettinetti, R., 2022. What are lake beaches made of? An assessment of plastic beach litter on the shores of Como Bay (Italy). Appl. Sci. 12, 5388. https://doi.org/10.3390/app12115388.

Bhagwat, G., O'Connor, W., Grainge, I., Palanisami, T., 2021. Understanding the fundamental basis for biofilm formation on plastic surfaces: role of conditioning films. Front. Microbiol. 12. https://doi.org/10.3389/fmicb.2021.687118.

Binda, G., Pozzi, A., Michetti, A.M., Noble, P.J., Rosen, M.R., 2020. Towards the understanding of hydrogeochemical seismic responses in karst aquifers: a retrospective meta-analysis focused on the Apennines (Italy). Minerals 10, 1058. https://doi.org/10.3390/min10121058.

Binda, G., Spanu, D., Monticelli, D., Pozzi, A., Bellasi, A., Bettinetti, R., Carnati, S., Nizzetto, L., 2021. Unfolding the interaction between microplastics and (trace) elements in water: a critical review. Water Res. 204, 117637. https://doi.org/10.1016/j.watres.2021.117637.

Binda, G., Faccini, D., Zava, M., Pozzi, A., Dossi, C., Monticelli, D., Spanu, D., 2022. Exploring the adsorption of Pb on microalgae-derived biochar: a versatile material for environmental remediation and electroanalytical applications. Chemosensors 10, 168. https://doi.org/10.3390/chemosensors10050168.

Binda, G., Carnati, S., Spanu, D., Bellasi, A., Hurley, R., Bettinetti, R., Monticelli, D., Pozzi, A., Nizzetto, L., 2023a. Selection of the optimal extraction protocol to investigate the interaction between trace elements and environmental plastic. J. Hazard. Mater. 131330. https://doi.org/10.1016/j.jhazmat.2023.131330.

Binda, G., Zanetti, G., Bellasi, A., Spanu, D., Boldrocchi, G., Bettinetti, R., Pozzi, A., Nizzetto, L., 2023b. Physicochemical and biological ageing processes of (micro)plastics in the environment: a multi-tiered study on polyethylene. Environ. Sci. Pollut. Res. 30, 6298–6312. https://doi.org/10.1007/s11356-022-22599-4.

Botté, A., Zaidi, M., Guery, J., Fichet, D., Leignel, V., 2022. Aluminium in aquatic environments: abundance and ecotoxicological impacts. Aquat. Ecol. 56, 751–773. https://doi.org/10.1007/s10452-021-09936-4.

Bradney, L., Wijesekara, H., Palansooriya, K.N., Obadamudalige, N., Bolan, N.S., Ok, Y.S., Rinklebe, J., Kim, K.-H., Kirkham, M.B., 2019. Particulate plastics as a vector for toxic trace-element uptake by aquatic and terrestrial organisms and human health risk. Environ. Int. 131, 104937. https://doi.org/10.1016/j.envint.2019.104937.

Campanale, C., Savino, I., Massarelli, C., Uricchio, V.F., 2023. Fourier transform infrared spectroscopy to assess the degree of alteration of artificially aged and environmentally weathered microplastics. Polymers 15, 911. https://doi.org/10.3390/polym15040911.

Cao, Y., Zhao, M., Ma, X., Song, Y., Zuo, S., Li, H., Deng, W., 2021. A critical review on the interactions of microplastics with heavy metals: mechanism and their combined effect on organisms and humans. Sci. Total Environ. 788, 147620. https://doi.org/10.1016/j.scitotenv.2021.147620.

Chen, C., Wei, F., Ye, L., Wang, Y., Long, L., Xu, C., Xiao, Y., Wu, J., Xu, M., He, J., Yang, G., 2022. Adsorption of Cu2+ by UV aged polystyrene in aqueous solution. Ecotoxicol. Environ. Saf. 232, 113292. https://doi.org/10.1016/j.ecoenv.2022.113292.

Chia, W.Y., Ying Tang, D.Y., Khoo, K.S., Kay Lup, A.N., Chew, K.W., 2020. Nature's fight against plastic pollution: algae for plastic biodegradation and bioplastics production. Environ. Sci. Ecotechnol. 4, 100065. https://doi.org/10.1016/j.ese.2020.100065.

Conan, P., Philip, L., Ortega-Retuerta, E., Odobel, C., Duran, C., Pandin, C., Giraud, C., Meistertzheim, A.-L., Barbe, V., Ter Hall, A., Pujo-Pay, M., Ghiglione, J.-F., 2022. Evidence of coupled autotrophy and heterotrophy on plastic biofilms and its influence on surrounding seawater. Environ. Pollut. 315, 120463. https://doi.org/10.1016/j.envpol.2022.120463.

Di Pippo, F., Venezia, C., Sighicelli, M., Pietrelli, L., Di Vito, S., Nuglio, S., Rossetti, S., 2020. Microplastic-associated biofilms in lentic Italian ecosystems. Water Res. 187, 116429. https://doi.org/10.1016/j.watres.2020.116429.

Djaoudi, K., Onrubia, J., Angel, T., Boukra, A., Guesnay, L., Portas, A., Barry-Martinet, R., Angeletti, B., Mounier, S., Lenoble, V., Briand, J.-F., 2022. Seawater copper content controls biofilm bioaccumulation and microbial community on microplastics. Sci. Total Environ. 814, 152278. https://doi.org/10.1016/j.scitotenv.2021.152278.

Duan, J., Li, Y., Gao, J., Cao, R., Shang, E., Zhang, W., 2022. ROS-mediated photoaging pathways of nano- and micro-plastic particles under UV irradiation. Water Res. 216, 118320. https://doi.org/10.1016/j.watres.2022.118320.

El Hadri, H., Gigault, J., Mounicou, S., Grassl, B., Reynaud, S., 2020. Trace element distribution in marine microplastics using laser ablation-ICP-MS. Mar. Pollut. Bull. 160, 111716. https://doi.org/10.1016/j.marpolbul.2020.111716.

Fan, X., Zou, Y., Geng, N., Liu, J., Hou, J., Li, D., Yang, C., Li, Y., 2021. Investigation on the adsorption and desorption behaviors of antibiotics by degradable MPs with or without UV ageing process. J. Hazard. Mater. 401, 123363. https://doi.org/10.1016/j.jhazmat.2020.123363.

Gaetke, L., 2003. Copper toxicity, oxidative stress, and antioxidant nutrients. Toxicology 189, 147–163. https://doi.org/10.1016/S0300-483X(03)00159-8.

Ganesan, S., Ruendee, T., Kimura, S.Y., Chawengkijwanich, C., Janjaroen, D., 2022. Effect of biofilm formation on different types of plastic shopping bags: structural and physico-chemical properties. Environ. Res. 206, 112542. https://doi.org/10.1016/j.envres.2021.112542.

Guan, J., Qi, K., Wang, J., Wang, W., Wang, Z., Lu, N., Qu, J., 2020. Microplastics as an emerging anthropogenic vector of trace metals in freshwater: significance of biofilms and comparison with natural substrates. Water Res. 184, 116205. https://doi.org/10.1016/j.watres.2020.116205.

Gundersen, P., Steinnes, E., 2003. Influence of pH and TOC concentration on Cu, Zn, Cd, and Al speciation in rivers. Water Res. 37, 307–318. https://doi.org/10.1016/S0043-1354(02)00284-1.

Herath, A., Salehi, M., 2022. Studying the combined influence of microplastics' intrinsic and extrinsic characteristics on their weathering behavior and heavy metal transport in storm runoff. Environ. Pollut. 308, 119628. https://doi.org/10.1016/j.envpol.2022.119628.

Hildebrandt, L., Nack, F.L., Zimmermann, T., Pröfrock, D., 2021. Microplastics as a Trojan horse for trace metals. J. Hazard. Mater. Lett. 2, 100035. https://doi.org/10.1016/j.hazl.2021.100035.

Holmes, L.A., Turner, A., Thompson, R.C., 2012. Adsorption of trace metals to plastic resin pellets in the marine environment. Environ. Pollut. 160, 42–48. https://doi.org/10.1016/j.envpol.2011.08.052.

Hurley, R., Kernchen, S., Binda, G., Carroccio, S., Consolaro, C., Cerruti, P., Löder, M., Laforsch, C., Briassoulis, D., Nizzetto, L., 2023. Production and characterisation of environmentally relevant microplastic reference materials for agricultural soils. Presented at the SETAC Europe 33 Annual Meeting, Dublin, Ireland.

Johan, P.D., Ahmed, O.H., Omar, L., Hasbullah, N.A., 2021. Phosphorus transformation in soils following co-application of charcoal and wood ash. Agronomy 11, 2010. https://doi.org/10.3390/agronomy11102010.

Johansen, M.P., Cresswell, T., Davis, J., Howard, D.L., Howell, N.R., Prentice, E., 2019. Biofilm-enhanced adsorption of strong and weak cations onto different microplastic sample types: use of spectroscopy, microscopy and radiotracer methods. Water Res. 158, 392–400. https://doi.org/10.1016/j.watres.2019.04.029.

Jung, M.R., Horgen, F.D., Orski, S.V., Rodriguez, C.V., Beers, K.L., Balazs, G.H., Jones, T.T., Work, T.M., Brignac, K.C., Royer, S.-J., Hyrenbach, K.D., Jensen, B.A., Lynch, J.M., 2018. Validation of ATR FT-IR to identify polymers of plastic marine debris, including those ingested by marine organisms. Mar. Pollut. Bull. 127, 704–716. https://doi.org/10.1016/j.marpolbul.2017.12.061.

Kalčíková, G., Skalar, T., Marolt, G., Jemec Kokalj, A., 2020. An environmental concentration of aged microplastics with adsorbed silver significantly affects aquatic organisms. Water Res. 175. https://doi.org/10.1016/j.watres.2020.115644.

Koelmans, A.A., Mohamed Nor, N.H., Hermsen, E., Kooi, M., Mintenig, S.M., De France, J., 2019. Microplastics in freshwaters and drinking water: critical review and assessment of data quality. Water Res. 155, 410–422. https://doi.org/10.1016/j.watres.2019.02.054.

Kotai, J., 1972. Instructions for Preparation of Modified Nutrient Solution Z8 for Algae. 11. Norwegian Institute for Water Research, Oslo, p. 5.

Lang, M., Yu, X., Liu, J., Xia, T., Wang, T., Jia, H., Guo, X., 2020. Fenton aging significantly affects the heavy metal adsorption capacity of polystyrene microplastics. Sci. Total Environ. 722, 137762. https://doi.org/10.1016/j.scitotenv.2020.137762.

Langford, K.H., Reid, M.J., Fjeld, E., Øxnevad, S., Thomas, K.V., 2015. Environmental occurrence and risk of organic UV filters and stabilizers in multiple matrices in Norway. Environ. Int. 80, 1–7. https://doi.org/10.1016/j.envint.2015.03.012.

Li, Yan, Wood, E., Kosa, G., Muzamil, B., Vogelsang, C., Holmstad, R., 2022b. A New Insight of phycoremediation Study: Using Filamentous Algae for the Treatment of Tertiary Municipal Wastewater. IntechOpen. https://doi.org/10.5772/intechopen.104253.

Li, Yuan, Wang, X., Wang, Y., Sun, Y., Xia, S., Zhao, J., 2022a. Effect of biofilm colonization on Pb(II) adsorption onto poly(butylene succinate) microplastic during its biodegradation. Sci. Total Environ. 833, 155251. https://doi.org/10.1016/j.scitotenv.2022.155251.

Liu, P., Shi, Y., Wu, X., Wang, H., Huang, H., Guo, X., Gao, S., 2021c. Review of the artificially-accelerated aging technology and ecological risk of microplastics. Sci. Total Environ. 768, 144969. https://doi.org/10.1016/j.scitotenv.2021.144969.

Liu, S., Shi, J., Wang, J., Dai, Y., Li, H., Li, J., Liu, X., Chen, X., Wang, Z., Zhang, P., 2021b. Interactions between microplastics and heavy metals in aquatic environments: a review. Front. Microbiol. 12. https://doi.org/10.3389/fmicb.2021.652520.

Liu, Z., Adyel, T.M., Miao, L., You, G., Liu, S., Hou, J., 2021a. Biofilm influenced metal accumulation onto plastic debris in different freshwaters. Environ. Pollut. 285, 117646. https://doi.org/10.1016/j.envpol.2021.117646.

Loo, A.E.K., Wong, Y.T., Ho, R., Wasser, M., Du, T., Ng, W.T., Halliwell, B., 2012. Effects of hydrogen peroxide on wound healing in mice in relation to oxidative damage. PLoS One 7, e49215. https://doi.org/10.1371/journal.pone.0049215.

Luo, H., Liu, C., He, D., Xu, J., Sun, J., Li, J., Pan, X., 2022. Environmental behaviors of microplastics in aquatic systems: a systematic review on degradation, adsorption, toxicity and biofilm under aging conditions. J. Hazard. Mater. 423, 126915. https://doi.org/10.1016/j.jhazmat.2021.126915.

Martínez, K.I., González-Mota, R., Soto-Bernal, J.J., Rosales-Candelas, I., 2021. Evaluation by IR spectroscopy of the degradation of different types of commercial polyethylene exposed to UV radiation and domestic compost in ambient conditions. J. Appl. Polym. Sci. 138, 50158. https://doi.org/10.1002/app.50158.

Miao, L., Yu, Y., Adyel, T.M., Wang, C., Liu, Z., Liu, S., Huang, L., You, G., Meng, M., Qu, H., Hou, J., 2021. Distinct microbial metabolic activities of biofilms colonizing microplastics in three freshwater ecosystems. J. Hazard. Mater. 403, 123577. https://doi.org/10.1016/j.jhazmat.2020.123577.

Nava, V., Leoni, B., 2021. A critical review of interactions between microplastics, microalgae and aquatic ecosystem function. Water Res. 188, 116476. https://doi.org/10.1016/j.watres.2020.116476.

Nava, V., Matias, M.G., Castillo-Escrivà, A., Messyasz, B., Leoni, B., 2021. Microalgae colonization of different microplastic polymers in experimental mesocosms across an environmental gradient. Glob. Chang. Biol. https://doi.org/10.1111/gcb.15989.

Ndungu, K., 2012. Model predictions of copper speciation in coastal water compared to measurements by analytical voltammetry. Environ. Sci. Technol. 46, 7644–7652. https://doi.org/10.1021/es301017x.

Nordstrom, D.K., 2015. Baseline and premining geochemical characterization of mined sites. Appl. Geochem. 57, 17–34. https://doi.org/10.1016/j.apgeochem.2014.12.010.

OriginLab Corporation, 2018. Origin, Version 2018 Northampton, MA, USA.

Palai, B., Mohanty, S., Nayak, S.K., 2021. A comparison on biodegradation behaviour of Polylactic acid (PLA) based blown films by incorporating Thermoplasticized starch (TPS) and poly (butylene succinate-co-Adipate) (PBSA) biopolymer in soil. J. Polym. Environ. 29, 2772–2788. https://doi.org/10.1007/s10924-021-02055-z.

Palsikowski, P.A., Kuchnier, C.N., Pinheiro, I.F., Morales, A.R., 2018. Biodegradation in soil of PLA/PBAT blends compatibilized with chain extender. J. Polym. Environ. 26, 330–341. https://doi.org/10.1007/s10924-017-0951-3.

Pete, A.J., Brahana, P.J., Bello, M., Benton, M.G., Bharti, B., 2023. Biofilm formation influences the wettability and settling of microplastics. Environ. Sci. Technol. Lett. 10, 159–164. https://doi.org/10.1021/acs.estlett.2c00728.

Pieristè, M., Chauvat, M., Kotilainen, T.K., Jones, A.G., Aubert, M., Robson, T.M., Forey, E., 2019. Solar UV-A radiation and blue light enhance tree leaf litter decomposition in a temperate forest. Oecologia 191, 191–203. https://doi.org/10.1007/s00442-019-04478-x.

Plöger, A., Fischer, E., Nirmaier, H.-P., Laglera, L.M., Monticelli, D., van den Berg, C.M.G., 2005. Lead and copper speciation in remote mountain lakes. Limnol. Oceanogr. 50, 995–1010. https://doi.org/10.4319/lo.2005.50.3.0995.

Qiongjie, W., Yong, Z., Yangyang, Z., Zhouqi, L., Jinxiaoxue, W., Huijuan, C., 2022. Effects of biofilm on metal adsorption behavior and microbial community of microplastics. J. Hazard. Mater. 424, 127340. https://doi.org/10.1016/j.jhazmat.2021.127340.

Ramsperger, A.F.R.M., Stellwag, A.C., Caspari, A., Fery, A., Lueders, T., Kress, H., Löder, M.G.J., Laforsch, C., 2020. Structural diversity in early-stage biofilm formation on microplastics depends on environmental medium and polymer properties. Water 12, 3216. https://doi.org/10.3390/w12113216.

Reineccius, J., Schönke, M., Waniek, J.J., 2022. Abiotic long-term simulation of microplastic weathering pathways under different aqueous conditions. Environ. Sci. Technol. acs.est.2c05746. https://doi.org/10.1021/acs.est.2c05746.

Richard, H., Carpenter, E.J., Komada, T., Palmer, P.T., Rochman, C.M., 2019. Biofilm facilitates metal accumulation onto microplastics in estuarine waters. Sci. Total Environ. 683, 600–608. https://doi.org/10.1016/j.scitotenv.2019.04.331.

Rozman, U., Kalčíková, G., 2022. Seeking for a perfect (non-spherical) microplastic particle – the most comprehensive review on microplastic laboratory research. J. Hazard. Mater. 424, 127529. https://doi.org/10.1016/j.jhazmat.2021.127529.

Rozman, U., Filker, S., Kalčíková, G., 2023. Monitoring of biofilm development and physicochemical changes of floating microplastics at the air-water interface. Environ. Pollut. 322, 121157. https://doi.org/10.1016/j.envpol.2023.121157.

Sanvito, F., Monticelli, D., 2021. Exploring bufferless iron speciation in seawater by competitive ligand equilibration-cathodic stripping voltammetry: does pH control really matter? Talanta 229, 122300. https://doi.org/10.1016/j.talanta.2021.122300.

Seeley, M.E., Song, B., Passie, R., Hale, R.C., 2020. Microplastics affect sedimentary microbial communities and nitrogen cycling. Nat. Commun. 11, 2372. https://doi.org/10.1038/s41467-020-16235-3.

Shan, E., Zhang, X., Li, J., Sun, C., Teng, J., Yang, X., Chen, L., Liu, Y., Sun, X., Zhao, J., Wang, Q., 2022. Incubation habitats and aging treatments affect the formation of biofilms on polypropylene microplastics. Sci. Total Environ. 831, 154769. https://doi.org/10.1016/j.scitotenv.2022.154769.

Silva Pinheiro, J.P., Bertacini de Assis, C., Sanches, E.A., Moreira, R.G., 2020. Aluminum, at an environmental concentration, associated with acidic pH and high water temperature, causes impairment of sperm quality in the freshwater teleost Astyanax altiparanae (Teleostei: Characidae). Environ. Pollut. 262, 114252. https://doi.org/10.1016/j.envpol.2020.114252.

Stabnikova, O., Stabnikov, V., Marinin, A., Klavins, M., Vaseashta, A., 2022. The role of microplastics biofilm in accumulation of trace metals in aquatic environments. World J. Microbiol. Biotechnol. 38, 117. https://doi.org/10.1007/s11274-022-03293-6.

Sun, Y., Yuan, J., Zhou, T., Zhao, Y., Yu, F., Ma, J., 2020. Laboratory simulation of microplastics weathering and its adsorption behaviors in an aqueous environment: a systematic review. Environ. Pollut. 265, 114864. https://doi.org/10.1016/j.envpol.2020.114864.

Tang, S., Lin, L., Wang, X., Feng, A., Yu, A., 2020. Pb(II) uptake onto nylon microplastics: interaction mechanism and adsorption performance. J. Hazard. Mater. 386, 121960. https://doi.org/10.1016/j.jhazmat.2019.121960.

Tong, C.Y., Chang, Y.S., Ooi, B.S., Chan, D.J.C., 2021. Physico-chemistry and adhesion kinetics of algal biofilm on polyethersulfone (PES) membrane with different surface wettability. J. Environ. Chem. Eng. 9, 106531. https://doi.org/10.1016/j.jece.2021.106531.

Turner, A., Filella, M., 2021. Hazardous metal additives in plastics and their environmental impacts. Environ. Int. 156, 106622. https://doi.org/10.1016/j.envint.2021.106622.

Wang, L., Zhang, J., Huang, W., He, Y., 2023. Laboratory simulated aging methods, mechanisms and characteristic changes of microplastics: a review. Chemosphere 315, 137744. https://doi.org/10.1016/j.chemosphere.2023.137744.

Wang, Q., Zhang, Y., Wangjin, X., Wang, Y., Meng, G., Chen, Y., 2020. The adsorption behavior of metals in aqueous solution by microplastics effected by UV radiation. J. Environ. Sci. (China) 87, 272–280. https://doi.org/10.1016/j.jes.2019.07.006.

Witzmann, T., Ramsperger, A.F.R.M., Wieland, S., Laforsch, C., Kress, H., Fery, A., Auernhammer, G.K., 2022. Repulsive interactions of eco-corona-covered microplastic particles quantitatively follow modeling of polymer brushes. Langmuir 38, 8748–8756. https://doi.org/10.1021/acs.langmuir.1c03204.

Worms, I., Simon, D., Hassler, C., Wilkinson, K.J., 2006. Bioavailability of trace metals to aquatic microorganisms: importance of chemical, biological and physical processes on biouptake. Biochimie 88, 1721–1731. https://doi.org/10.1016/j.biochi.2006.09.008.

Wright, R.J., Erni-Cassola, G., Zadjelovic, V., Latva, M., Christie-Oleza, J.A., 2020. Marine plastic debris: a new surface for microbial colonization. Environ. Sci. Technol. 54, 11657–11672. https://doi.org/10.1021/acs.est.0c02305.

Xie, L., Solhaug, K.A., Song, Y., Johnsen, B., Olsen, J.E., Tollefsen, K.E., 2020. Effects of artificial ultraviolet B radiation on the macrophyte Lemna minor: a conceptual study for toxicity pathway characterization. Planta 252, 86. https://doi.org/10.1007/s00425-020-03482-3.

Xie, M., Huang, J.-L., Lin, Z., Chen, R., Tan, Q.-G., 2021. Field to laboratory comparison of metal accumulation on aged microplastics in coastal waters. Sci. Total Environ. 797, 149108. https://doi.org/10.1016/j.scitotenv.2021.149108.

Yu, Y., Miao, L., Adyel, T.M., Waldschläger, K., Wu, J., Hou, J., 2023. Aquatic plastisphere: interactions between plastics and biofilms. Environ. Pollut. 322, 121196. https://doi.org/10.1016/j.envpol.2023.121196.

Zheng, M., Wu, P., Li, L., Yu, F., Ma, J., 2023. Adsorption/desorption behavior of ciprofloxacin on aged biodegradable plastic PLA under different exposure conditions. J. Environ. Chem. Eng. 11, 109256. https://doi.org/10.1016/j.jece.2022.109256.

Zhou, J., Chen, H., Guo, Y., Chen, Q., Ren, H., Tao, Y., 2022. Changes in metal adsorption ability of microplastics upon loss of calcium carbonate filler masterbatch through natural aging. Sci. Total Environ. 832, 155142. https://doi.org/10.1016/j.scitotenv.2022.155142.

Zvekic, M., Richards, L.C., Tong, C.C., Krogh, E.T., 2022. Characterizing photochemical ageing processes of microplastic materials using multivariate analysis of infrared spectra. Environ Sci Process Impacts 24, 52–61. https://doi.org/10.1039/d1em00392e.